Author/s:
Fabian, SG;Gallagher, SJ;De Vleeschouwer, D

Title:
Benthic foraminiferal population dynamics at the Goban Spur off Southwest Ireland reveal glacial-interglacial bottom water ventilation and organic flux variability over the last 420,000 years

Date:
2025-01-01

Citation:
Fabian, S. G., Gallagher, S. J. & De Vleeschouwer, D. (2025). Benthic foraminiferal population dynamics at the Goban Spur off Southwest Ireland reveal glacial-interglacial bottom water ventilation and organic flux variability over the last 420,000 years. Marine Micropaleontology, 194, https://doi.org/10.1016/j.marmicro.2024.102432.

Persistent Link:
https://hdl.handle.net/11343/354894

Marine Micropaleontology 194 (2025) 102432

Contents lists available at ScienceDirect

Marine Micropaleontology

journal homepage: www.elsevier.com/locate/marmicro

Research paper

Benthic foraminiferal population dynamics at the Goban Spur off Southwest Ireland reveal glacial-interglacial bottom water ventilation and organic flux variability over the last 420,000 years

Stanislaus Glenndy Fabian [a,*], Stephen J. Gallagher [a], David De Vleeschouwer [b]

[a] Earth and Atmospheric Sciences, McCoy Building, Corner Swanston & Elgin Streets, The University of Melbourne, Parkville, VIC 3010, Australia
[b] Institute of Geology and Paleontology, University of Münster, Corrensstr 24, 48149 Münster, Germany

ARTICLE INFO

Keywords:
Benthic Foraminifera
North Atlantic
Quarternary
Goban Spur
DSDP Site 548
Mediterranean Outflow Water

ABSTRACT

Benthic foraminiferal assemblages from Deep Sea Drilling Project (DSDP) Site 548 on the Goban Spur off southwestern Ireland shed light on the changes in bottom water oxygenation and organic matter flux to the sea floor during the late Quaternary. Correlations of benthic foraminiferal $\delta^{18}O$ values, the relative abundance of *Neogloboquadrina pachyderma* (%NP), and Ice Rafted Debris (IRD) concentration to global and regional and North Atlantic datasets suggest the upper 60 m of DSDP Site 548 extend to 420,000 years. Downcore variations of >63 μm benthic foraminifera assemblages, abundance, and diversity reveal changes in dissolved oxygen concentration and organic fluxes to the seafloor related to glacial-interglacial cyclicity. *Cassidulina laevigata* and low dissolved oxygen indicator taxa such as *Bolivina* spp. and *Globobulimina* spp. characterised colder climates associated with lighter benthic $\delta^{13}C$ values, suggesting minimal organic flux and/or weaker bottom water ventilation. In contrast, warmer interglacials are typified by heavier benthic $\delta^{13}C$, increased $\%CaCO_3$, common high dissolved oxygen indicator taxa such as *Globocassidulina subglobosa* and phytodetritus sensitive taxa such as *Alabaminella weddellensis* and *Epistominella exigua*, suggest a more ventilated bottom water and increased organic fluxes to the seafloor, possibly associated with the invigoration of the Mediterranean Outflow Water (MOW).

1. Introduction

Foraminiferal assemblage analysis of marine sedimentary cores is commonly used for Quaternary palaeoclimatic and palaeoceanographic reconstructions of the North Atlantic (Thomas et al., 1995; Rüggeberg et al., 2007; O'Reilly et al., 2022). Planktonic foraminiferal assemblage analyses using the relative abundance of the polar water indicator *Neogloboquadrina pachyderma* (%NP)(van Kreveld, 1996; Kucera, 2007) and other taxa combined with foraminiferal Mg/Ca elemental ratios are used for estimating Sea Surface Temperatures (SST) (Lear et al., 2015; Vázquez Riveiros et al., 2016), and the relative position of the Polar Front (Eynaud et al., 2009; Bashirova et al., 2014). Benthic foraminiferal assemblages may serve as proxies for palaeoproductivity (Thomas et al., 1995; Thomas and Gooday, 1996; Saraswat et al., 2011), bottom water oxygenation (Kaiho, 1994; Kranner et al., 2022), the dynamics of bottom water masses in the North Atlantic (Schnitker, 1980; Schönfeld, 1997; Schönfeld and Zahn, 2000; Schönfeld, 2002), and when combined with stable isotope and geochemical data, these assemblages have been used to interpret Quaternary climatic variability (Brückner, 2007; Diz et al., 2007; Depuydt et al., 2022). However, equivalent deep-sea benthic foraminifera assemblage analyses of North Atlantic Quaternary marine archives, especially those covering periods older than the last glacial cycle, are relatively sparser than their planktonic counterpart.

The TROX (**TR**ophic-**OX**ygenation) model (Jorissen et al., 1995) describes benthic foraminifera's likely microhabitat depth limit based on the nutrient and dissolved oxygen availability on the seafloor and in the sediment. In this model, Jorissen et al. (1995) suggest that nutritional scarcity limits the depth of benthic microhabitats in an oligotrophic environment. In contrast, the extent of dissolved oxygen availability controls the depth limit of benthic microhabitats within eutrophic environments. Based on dissolved oxygen concentrations, the environment may be classified as dysoxic, suboxic and oxic (Table 1). Kranner et al. (2022) modified the TROX model to explain the depth habitat of benthic foraminifera relative to the bottom and pore water oxygenation. Based on their model, oxic epifaunal taxa dominate a well-oxygenated seabed. The benthic foraminiferal assemblages in

* Corresponding author.
E-mail addresses: stglenn49@gmail.com (S.G. Fabian), sjgall@unimelb.edu.au (S.J. Gallagher), ddevlees@uni-muenster.de (D. De Vleeschouwer).

https://doi.org/10.1016/j.marmicro.2024.102432
Received 22 May 2024; Received in revised form 9 December 2024; Accepted 10 December 2024
Available online 16 December 2024

Table 1
EBFOI species classification based on Kranner et al. (2022) and Kaiho (1994).

Oxygen Condition	Oxygen level (mL/L)	EBFOI	Benthic foraminifera assemblages	Indicator Species
High oxic	3.0–6.0	50–100	Dysoxic, suboxic, high ratios of oxic indicators	*Cibicides* spp., *Cibicidoides* spp., *Globocassidulina subglobosa, Pyrgo* spp., *Quinqueloculina* spp., *Triloculina* spp.
Low oxic	1.5–3.0	0–50	Dysoxic, suboxic, and low ratios of oxic indicators	
Suboxic	0.3–1.5	−40–0	Dysoxic and high ratios of suboxic indicators	*Alabaminella* spp., *Astrononion pusillum, Bulimina striata, Cancris* spp., *Cassidulina* spp., *Favocassidulia favus, Fissurina* spp., *Gyroidina* spp., *Gyroinoides* spp., *Hoeglundina elegans, Lagena* spp., *Lenticulina* spp., *Melonis* spp., *Nonion* spp., *Oridorsalis* spp., *Pullenia* spp., *Sphaeroidinia bulloides, Trifarina* spp. *Uvigerina* spp., *Valvulineria* spp.
Dysoxic	0.3–0.1	−50 to −40	Dysoxic and low ratios of suboxic indicators	*Bolivina* spp., *Bulimina aculeata, Bulimina exilis, Chilostomella oolina, Cribroelphidium excavatum, Globobulimina* spp., *Nonionella* spp.
Anoxic	0.0–0.1	−55	Barren of benthic foraminfera	

suboxic environments are typically a mixture of oxic epifaunal, suboxic shallow and deep infaunal taxa with minor dysoxic deep infaunal taxa (Table 1). In dysoxic environments, the absence of oxic epifaunal taxa promotes a more suitable environment for suboxic infaunal taxa. Further, as the dissolved oxygen concentration decreases, the benthic foraminiferal assemblages become dominated by dysoxic deep infaunal taxa, which may migrate to shallower depths. This model also suggests the absence of benthic foraminifera associated with anoxia. Thus, benthic foraminiferal assemblages are sensitive to changes in bottom water oxygenation levels and are good proxies for changes in bottom water ventilation.

The classification of benthic foraminiferal oxygenation indicator species (Table 1), based on the pioneering work by Kaiho (1994) and improved recently by Kranner et al. (2022), is used to classify benthic foraminiferal taxa. The Benthic Foraminifera Oxygenation Index (BFOI) is calculated using the abundance of oxic, suboxic and dysoxic taxa corresponding to relative dissolved oxygen levels (Kaiho, 1994) (Table 1). The Enhanced BFOI (EBFOI) was modified by Kranner et al. (2022) by including the relative abundance of agglutinated foraminifera and considering the difference between bottom water and pore water oxygenation. These authors also reclassified some oxic taxa previously considered suboxic indicators by Kaiho (1994) (see also Table 1).

Detrital matter from surface phytoplankton (phytodetritus) (Turner, 2015) is an important nutrient source for the North Atlantic seafloor (Rice et al., 1994). In the region, the relative abundance of benthic foraminiferal taxa such as *Epistominella exigua* and *Alabaminella weddellensis* are related to increased seasonality of organic matter fluxes and primary productivity (Sun et al., 2006), organic flux to the seafloor (Gooday, 1993) and surface plankton blooms (Thomas et al., 1995). Meanwhile, the abundance of *Globocassidulina subglobosa* negatively correlates to seasonality (Sun et al., 2006). Thus, estimates of organic matter flux to the seafloor may be inferred from the distribution of these phytodetritus indicator species.

Thus, this work aims to present a long-term record of the >63 μm benthic foraminiferal assemblages from the upper 60 m of Deep Sea Drilling Project (DSDP) Site 548 (Fig. 1) and interpret their variations in association with changes in bottom water oxygenation levels and organic matter fluxes to the seafloor through the glacial-interglacial cycle. This work extends the palaeoenvironmental records of the Goban Spur of Fabian et al. (2023), which discusses a palaeoclimatic record based on planktonic foraminiferal assemblages for the past 250,000 years. This study is significant as it offers a long-term record of deep-sea benthic foraminiferal response to changes in bottom water oxygenation and organic flux levels associated with the glacial-interglacial cycle whilst extending the age model for DSDP Site 548 and improving the relatively sparse long-term benthic foraminiferal assemblages record around the North Atlantic record particularly those older than the last glacial cycles. The combination of multi-species benthic $\delta^{18}O$ measurements, the relative abundance of the planktonic foraminifera *Neogloboquadrina pachyderma* (%NP), Ice Rafted Debris concentration (IRD), and calcium carbonate (%$CaCO_3$) data are used to extend the DSDP Site 548 age model of Fabian et al. (2023). Further, this work also uses EBFOI (Kranner et al., 2022) to estimate changes in bottom water ventilation and utilises variations of benthic foraminiferal assemblages, abundance, diversity and benthic $\delta^{13}C$ to interpret their responses to changes in bottom water conditions associated with glacial-interglacial cycles, including organic matter flux at the Goban Spur for the past 420,000 years.

2. Setting

DSDP Site 548 (48°54.95′N;12°09.84′W, 1256 m water depth) (Fig. 1) was cored during the DSDP Leg 80, accompanied by a downhole wireline logging at DSDP Site 548-A (48°54.93′N;12°09.87′W), 30 m west of DSDP Site 548 (De Graciansky et al., 1985b). The upper 60 m of DSDP Site 548 is divided into 2 subunits, Subunit U1a and U1b (De Graciansky et al., 1985a), with an unconformity surface relating to a local slope failure defining the border (Delivet et al., 2016; Fabian et al., 2023). Presently, three water masses of the Northeastern Atlantic Ocean are present near the study area: Eastern North Atlantic Central Water (ENACW) at ~500 m water depth, Mediterranean Outflow Water (MOW) centred at ~800 m, and Labrador Sea Water (LSW) at ~1800 m (Delivet et al., 2016) (Fig. 1). The north-flowing MOW forms a thermohaline geostrophic current flowing inside the Porcupine Sea Bight (Fig. 1) with an average velocity from 2 to 10 m/s (Delivet et al., 2016). The relative strength of the MOW controls contourite deposition along the eastern continental margin of the North Atlantic Ocean (Gonthier et al., 1984; Schönfeld, 1997; Kaboth et al., 2017). Presently, the lower part of MOW is the bottom water mass bathing DSDP Site 548 (Fig. 1) (Delivet et al., 2016), and thus, its strength affects the contourite deposition at the Goban Spur (Fabian et al., 2023).

3. Material and methods

3.1. Core analyses

The upper 60 m at DSDP Core 548 were logged (Fig. 2) and sampled for microfossils and coarse lithic clasts. Carbonate content (%$CaCO_3$) measurements of 118 samples from the core used a modified volumetric technique of Hulsemann (1966) (cf. Wallace et al., 2002). This study defines coarse lithic clasts as all non-biogenic grains >150 μm. Their presence at DSDP Site 548 is interpreted as products of iceberg calving, primarily hailing from the British Irish Ice Sheet (Fabian et al., 2023). Lithic grain census counts were done on splits of microfossil residues, yielding a minimum of 200 counts of >150 μm lithic clasts.

3.2. Foraminiferal analyses

118 samples from the upper 60 m at DSDP Site 548 were analysed for

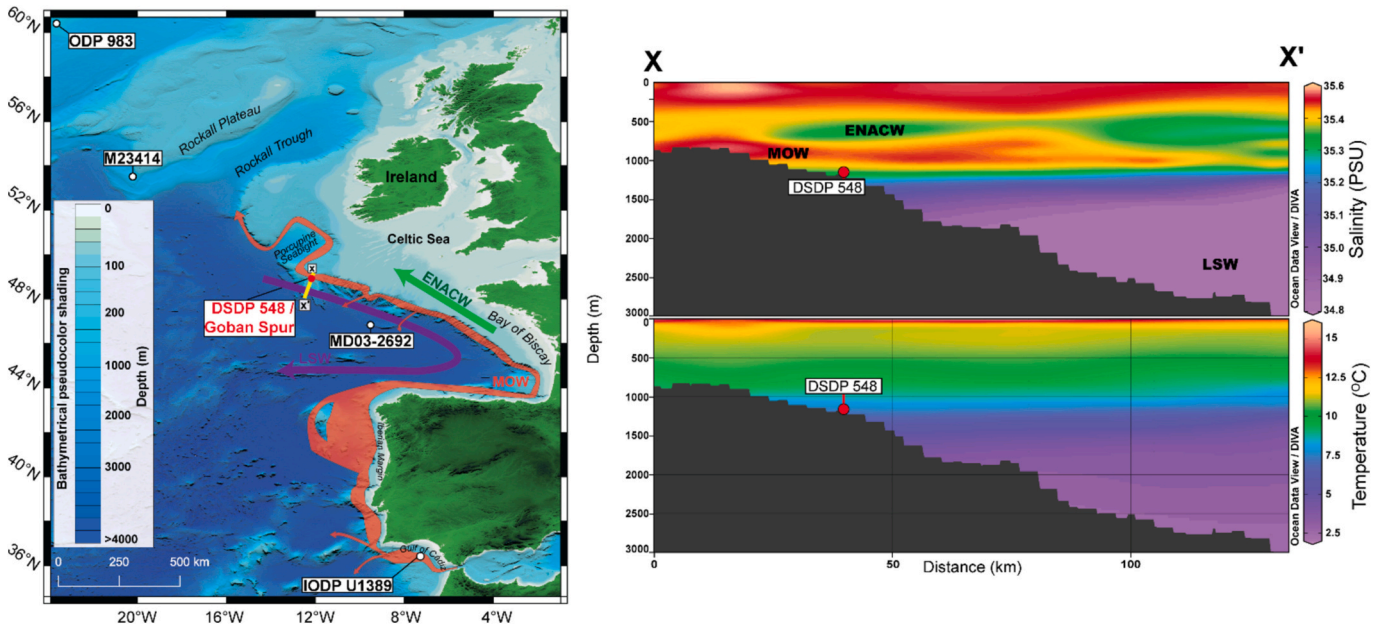

Fig. 1. Map of MOW mean flow path (Delivet et al., 2016) and relevant core sites, including DSDP Site 548(De Graciansky et al., 1985a), ODP (Ocean Drilling Program) Site 983 (Barker et al., 2019), MD03–2692 (Mojtahid et al., 2005), M23414 (Kandiano, 2009) and IODP (Integrated Ocean Drilling Program) Site U1389 (Kaboth-Bahr et al., 2018). Vertical salinity and temperature profile at the Goban Spur, designation of water masses and the location of DSDP Site 548 are modified after Delivet et al. (2016), and the vertical profiles are drawn using the Ocean Data View (ODV) software package of Schlitzer (2023).

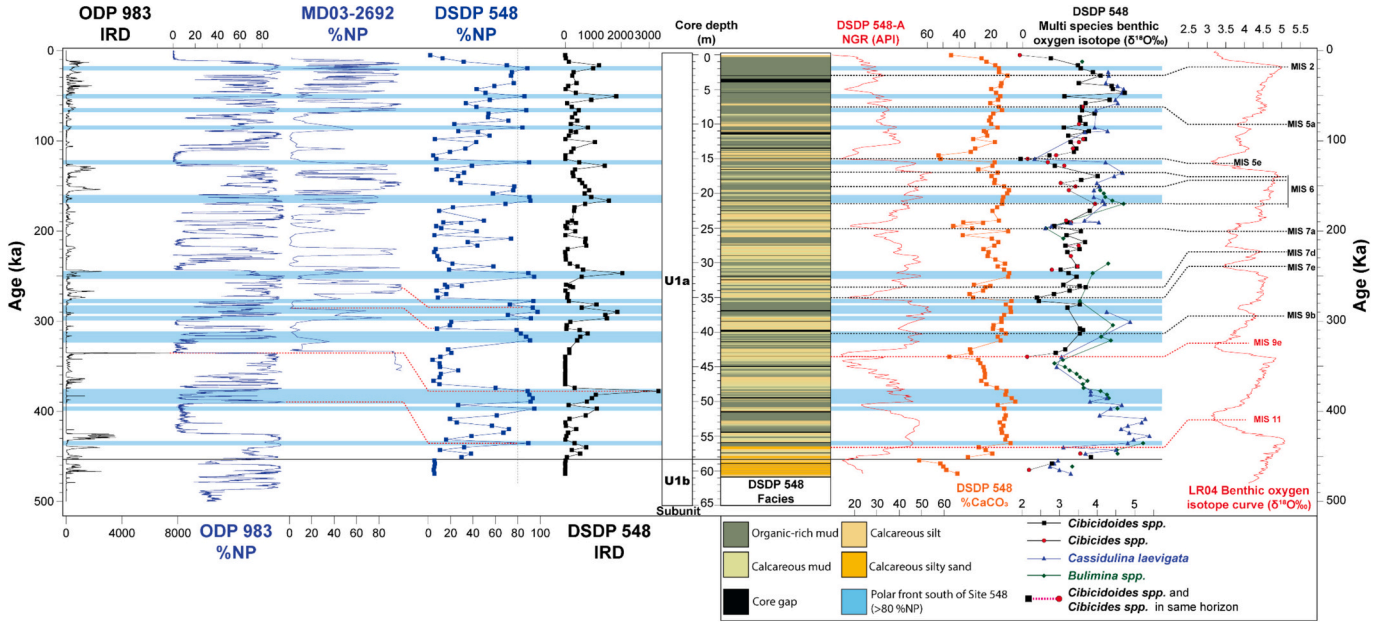

Fig. 2. Stratigraphic correlation for DSDP Site 548, extended from Fabian et al. (2023), based on IRD concentration and *Neogloboquadryna pachyderma* (%NP) values between DSDP Site 548 ODP Site 983 and Core MD03–2692 and lithofacies, calcium carbonate concentration, NGR (De Graciansky et al., 1985a) and benthic oxygen isotope data of DSDP Site 548 to the LR04 stack of Lisiecki and Raymo (2005). Light blue shading indicates intervals with more than 80 % NPS, interpreted to signify the presence of the polar front at or south of DSDP Site 548. The 0.45 Ma age boundary is from (Delivet et al., 2016). Black dashed lines indicate age correlation from Fabian et al. (2023), and red dashed lines indicate those from this work. (For interpretation of the references to colour in this figure legend, the reader is referred to the web version of this article.)

benthic foraminiferal assemblages and the relative abundance of the polar water indicator planktonic foraminifera *Neogloboquadrina pachyderma* (%NP); the same samples are also used for the lithic grain census counts. The samples were dried, weighed, and chemically disaggregated using hydrogen peroxide, wet-sieved using a 63 μm sieve and the residue dried. The residues were split until an aliquot of around 100–200 specimens of benthic foraminifera were obtained. The benthic assemblage census counts were then carried out on this fraction.

3.2.1. *Selection of size fraction for benthic foraminiferal analyses*

Due to their low yield at DSDP Site 548, this work documented benthic foraminifera distribution in the >63 μm size fraction, and planktonic foraminiferal species were documented from the >150 μm size fraction. Benthic foraminiferal analyses on >63 μm fraction are not

typically carried out on North Atlantic Quaternary cores. However, Thomas et al. (1995) demonstrated the potential for this finer-size fraction to reveal changes in seafloor organic flux, and Schönfeld et al. (2010) maintained that the >63 μm size fraction may be used in the presence of a limited sample size (cf. Fontanier, 2006). In addition, the smaller size fraction may yield a better record of the smaller opportunistic phytodetritus indicators taxa such as *Epistominella exigua* and *Alabaminella weddellensis* (Thomas et al., 1995; Thomas and Gooday, 1996; Depuydt et al., 2023) The benthic assemblages were compared to modern analogues and other downcore data from ODP Site 983 (Barker et al., 2019), MD03–2692 (Mojtahid et al., 2005) and IODP Site U1389 (Kaboth et al., 2017) (Fig. 1).

3.2.2. Foraminiferal abundance

BFAR (Benthic Foram Accumulation Rate) is commonly used to measure the relative benthic abundance in marine cores (Zahn et al., 1986; Thomas et al., 1995). However, it was not possible to get these values as they require Dry Bulk Density (DBD) estimates (Clemens et al., 1987), and DBD measurements were not carried out during DSDP Leg 80 (De Graciansky et al., 1985b). Therefore, this work uses the benthic foraminiferal abundance per gram of dry sediment. Since the sediments of DSDP Site 548 are at >1200 m depth, shallower water benthic taxa such as *Cribroelphidium excavatum* (cf. Murray, 2006) are excluded from our assemblage analyses as these taxa do not represent the seafloor conditions at DSDP Site 548.

3.2.3. Foraminiferal diversity

Benthic foraminiferal diversity is represented as ENS (Effective Number of Species) (Jost, 2006). Due to the low benthic foraminifera abundance in some of the samples and limited species identification, benthic foraminiferal diversity is represented qualitatively as very low, low, moderate and high; a further explanation of this matter is discussed in (Supplementary Material-S1). Despite the lower resolution of this data, a gross sense of species diversity would help paint a more comprehensive picture of the response of benthic foraminiferal communities to past changes in organic matter fluxes and bottom-water oxygenation.

3.2.4. Enhanced Benthic Foraminifera Oxygenation Index (EBFOI) calculation

This study uses EBFOI to estimate past dissolved oxygen levels in the bottom water based on the proportion of indicator species (Table 1) in the benthic foraminiferal assemblages. The equation to calculate EBFOI is as follows:

$$EBFOI = \frac{100\left(\frac{O}{\left(O+D+\frac{S}{2}\right)}\right) + 50\left(\frac{S}{(S+D)} - 1 + \frac{O}{2}\right)}{2} \quad (1)$$

Where:
O: proportion of oxic indicator species.
S: proportion of suboxic indicator species.
D: proportion of dysoxic indicator species.

3.3. Benthic foraminiferal stable isotope analyses

Carbon and oxygen isotope ($\delta^{13}C$ and $\delta^{18}O$) measurements on >150 μm infaunal (*Cassidulina laevigata* and *Bullimina* spp.) and epifaunal (*Cibicides* spp., and *Cibicidoides* spp.) benthic foraminifers were carried out at the Institute of Geology and Paleontology at the University of Münster (Germany) using a GasBench connected to a ThermoScientific Delta V Plus mass spectrometer via a ConFlo III interface. Individual measurements were carried out on sonicated foraminiferal tests, with sample weights between 50 and 180 μg per analysis. Results are reported in the standard delta notation as per mil difference relative to V-PDB (Vienna Pee Dee Belemnite). Accuracy was checked against two in-house standards, as well as against NBS-19. Reproducibility, as determined through replicate measurements of standards that were not used for the correction scheme, was better than ±0.16 ‰ for $\delta^{18}O$ and ± 0.06 ‰ for $\delta^{13}C$ (2σ).

4. Results

4.1. DSDP Site 548 Age Model

The age model used in this study extends those published by Fabian et al. (2023) (Fig. 2, Table 2), which covers it to 250 ka. The age model is constructed using benthic foraminiferal $\delta^{18}O$ values supported by NGR and %CaCO3 correlation to the LR-04 curve (Lisiecki and Raymo, 2005) (Fig. 4). Supplementary tie points are acquired from %NP and IRD comparison to cores ODP 983 (Barker et al., 2019) and MD03–2692 (Mojtahid et al., 2005) (Fig. 5). Further, one datum from Delivet et al. (2016), which indicates the boundary between Subunit U1a and U1b, defined by an unconformity surface related to a local slope failure, is used to refine the age model (Fig. 2, Table 2).

4.2. Benthic foraminiferal abundance

Benthic foraminiferal abundance is lower during the glacial periods, with minimum abundance associated with glacial level (>80 %) of %NP (Fig. 3). Benthic abundance maxima at MIS 11c decreased until a minimum at ~390 ka and remained low until the end of MIS 10 (Termination 4). Their abundance rapidly increased, reaching a maximum at MIS 9 and decreasing to a minimum by the end of MIS 8 (Termination 3). MIS 7 is typified by higher benthic foraminiferal abundance with maxima associated with MIS 7e, 7c, and 7a interglacials, except for a minimum associated with the MIS 7d stadial. Benthic abundance was low during MIS 6 with a minimum at ~171 ka. A benthic abundance maximum at MIS 5e is followed by a decrease in abundance to the end of

Table 2
Age tie points used to construct the age model.

Depth (m)	Age (ka)	Note	Source	References
0.28	11.65	Holocene Mud end	DSDP Site 548 initial report	De Graciansky et al. (1985a); Fabian et al. (2023)
3	18	LGM	LR-04 benthic oxygen isotope	Lisiecki and Raymo (2005); Railsback et al. (2015); Fabian et al. (2023)
7.52	82	5a		
15.02	125	5e		
17	140	6a		
21.06	155.2	NPS peak	MD03–2692	Fabian et al. (2023); Mojtahid et al. (2005)
21.5	171	MIS 6d	LR-04 benthic oxygen isotope	Lisiecki and Raymo (2005); Fabian et al. (2023); Railsback et al. (2015)
25.02	200	7a		
32.02	223	7d		
35.02	240	7e		
36.49	263	NPS peak	MD03–2692	Mojtahid et al. (2005); Fabian et al. (2023)
39.5	283	NPS low		
40.19	294	MIS 9b	LR-04 benthic oxygen isotope	Lisiecki and Raymo (2005), Railsback et al. (2015)
42.5	324	MIS 9		Lisiecki and Raymo (2005), Railsback et al. (2015)
48.51	335.6	NPS peak and IRD	MD03–2693, ODP Site 983	Mojtahid et al. (2005), Barker et al. (2019)
56.03	390.1	NPS peak	ODP Site 983	Barker et al. (2019)
56.61	405	MIS 11	LR-04 benthic oxygen isotope	Lisiecki and Raymo (2005), Railsback et al. (2015)
58.4	450	Unit boundary	DSDP 548 initial report, seismofacies	De Graciansky et al. (1985a), Delivet et al. (2016)

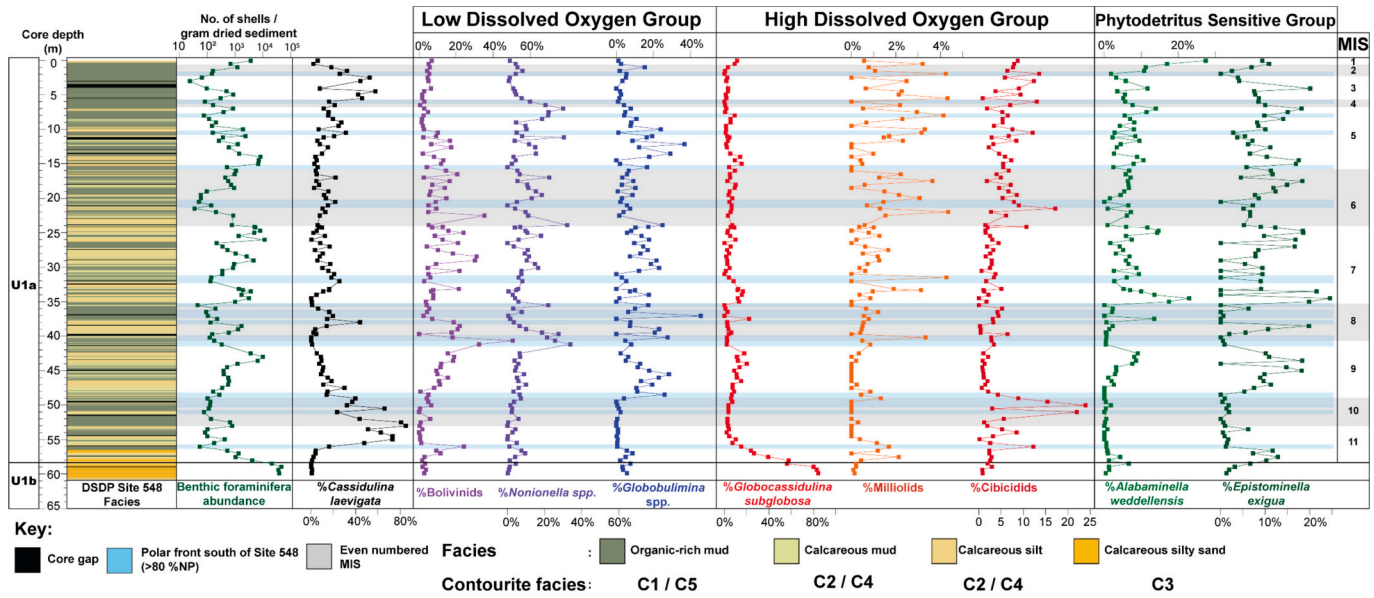

Fig. 3. Downcore variations in benthic foraminiferal abundance, major benthic taxa and facies of DSDP Site 548. Light blue shading indicates intervals where the polar front was south of Site 548 (>80 % NP), and grey shading indicates glacial Marine Isotope Stages (MIS). (For interpretation of the references to colour in this figure legend, the reader is referred to the web version of this article.)

MIS 2. Following Termination 1, benthic foraminiferal abundance increased to the present. Benthic foraminiferal diversity was higher during the interglacial than the glacial periods. Variations in diversity were minimal from MIS 11 to MIS 4, whereas it was more marked from MIS 3 to MIS 1, with peak abundance diversity at ~12.2 ka.

4.3. Benthic foraminiferal assemblages

The most common benthic taxa at DSDP Site 548 include *Cassidulina laevigata* and *Globocassidulina subglobosa*. Additional low dissolved oxygen assemblages include *Bolivina* spp., *Bulimina* spp., and *Globobulimina* spp. (See Supplementary Data S2). Taxa sensitive to phytodetritus input include *Alabaminella weddellensis* and *Epistominella exigua* (Thomas and Gooday, 1996) (Fig. 3). The downcore variability of these taxa often corresponds to changes in the sedimentary facies. Taxa indicative of low dissolved oxygen concentrations and *C. laevigata* dominate the low foraminiferal abundance mud-dominated facies (Fig. 3). In contrast, the phytodetritus sensitive taxa and *G. subglobosa* dominate silt-sand facies marked by higher benthic and planktic foraminiferal abundance (Fig. 3). The benthic eco groups and their relationship to facies and benthic foraminifera at DSDP Site 548 is summarised in (Table 3).

The low dissolved oxygen indicator group at its acme comprises 80 % of the total benthic population, with *Bolivina* spp. being the most common species in the group throughout the record (Fig. 4). Near the middle of MIS 11 (~410 ka), this group comprises ~40 % of the benthic foraminifera assemblage, rapidly decreasing in abundance by MIS 10. Subsequently, they reached a maximum at the MIS 9/8 transition (~300 ka) and another maximum near the end of MIS 8 (Termination 3). Low dissolved oxygen indicator taxa were rare in MIS 7 (243–191 ka), aside from a maximum (60 %) at ~213 ka. Low dissolved oxygen indicator taxa were abundant at the start of MIS 6 (~191 ka), reaching a minimum by MIS 5e (~122 ka). Thereafter, a maximum at MIS 5d (~109 ka) is followed by a decrease in abundance to the Holocene, with a minor peak associated at ~14 ka.

Cassidulina laevigata are abundant during the MIS 11 to 10 transition (Fig. 4), reaching a maximum of 85 % of the total benthic population by ~368 ka. Subsequently, the abundance decreased, becoming rare during the transition from MIS 9 to MIS 8 (~ 300 ka). Their abundance peaks in the middle of MIS 8 (~277 ka) are associated with a minimum abundance of the low dissolved oxygen indicator group before becoming rare until MIS 5. Minor peaks are associated with the MIS 7d (~223 ka) stadial and MIS 6 (~153 ka and 140 ka). Subsequently, *C. laevigata* abundance increases gradually to the end of MIS 2, with maxima at ~39 ka and ~ 18 ka. By MIS 1, *C. laevigata* becomes rare, comprising less than 10 % of the benthic foraminiferal assemblage.

The high dissolved oxygen indicator group is dominated by *Globocassidulina subglobosa*, particularly at intervals associated with strong interglacial conditions such as at MIS 1, 5e, 7e, 9 and 11 (Fig. 7), with a maximum at ~417 ka (MIS 11) (~60 %). Subsequently, this group became rarer to the end of MIS 8, where they were absent. After this, the high dissolved oxygen group's abundance gradually increases up to the Holocene, with more minor peaks (~25 %) at ~275 ka, 175 ka, and ~

Table 3
Common benthic foraminifera and their respective eco groups associated with the different facies and benthic foraminiferal abundance at DSDP Site 548.

Benthic eco group/species	Members	References	DSDP Site 548	
			Facies	Benthic abundance
High dissolved oxygen group	*Cibicides* spp., *Cibicidoides* spp., *Globocassidulina subglobosa, Pyrgo* spp., *Quinqueloculina* spp., *Triloculina* spp.	Kaiho (1994), Kranner et al. (2022)	Calcareous silt-sand	High
Low dissolved oxygen group	*Bolivina* spp., *Bulimina aculeata, Bulimina exilis, Chilostomella oolina, Cribroelphidium excavatum, Globobulimina* spp., *Nonionella* spp.		Organic-rich mud	Low
Phytodetritus sensitive group	*Alabaminella weddellensis, Epistominella exigua*	Thomas and Gooday (1996)	Calcareous silt-sand	Moderate-high
Cassidulina laevigata			Organic-rich mud	Low

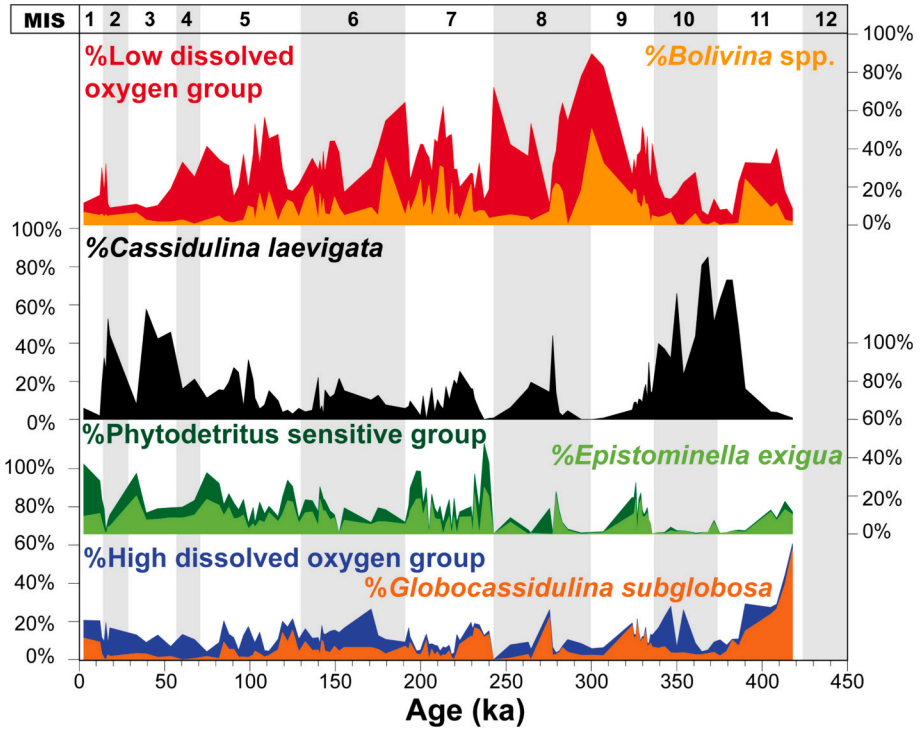

Fig. 4. The distribution of *Cassidulina laevigata*, major benthic ecogroups and the most abundant species within each eco group at DSDP Site 548, expressed as a percentage of the total benthic foraminifera. Grey shading indicates even-numbered MIS.

87 ka. The abundance of *G. subglobosa* positively correlates to %$CaCO_3$.

Maxima of species sensitive to phytodetrital input are present during MIS 11 (Hoxnian) and 9 (Aveley) interglacial periods. In contrast, the glacial MIS 10 is marked by rare phytodetritus sensitive taxa that became absent at ~336 ka. These taxa are rarer during MIS 8, with a maximum of ~20 % at ~329 ka. During MIS 7, the maximum of this group is associated with MIS 7e (~240 ka), whereas the minimum occurred during MIS 7d (~223 ka). From MIS 6 to MIS 1, phytodetritus abundance increased during warmer periods with peaks at ~122 ka (MIS 5e) and ~ 33 ka (MIS 3). Conversely, minima were often associated with stadial periods, such as their near absence during MIS 6 (~153 ka) and late MIS 2 or Termination 1 (~16 ka).

4.4. Enhanced Benthic Foraminifera Oxygenation Index (EBFOI)

Based on their oxygen requirements, the benthic foraminiferal assemblages were classified into oxic, suboxic, and dysoxic taxa (Kaiho, 1994; Kranner et al., 2022) (Table 1). Suboxic taxa were the most common, reaching a maximum (80 %) at 368 ka. EBFOI values vary markedly from low oxic (3–1.5 mL/L) to suboxic (1.5–0.3 mL/L) throughout the record, with a maximum at ~417 ka, during MIS 11 and a minimum near the end of MIS 8 (Termination 3) (Fig. 5). In general, after MIS 11, the EBFOI value decreased to the end of MIS 9 before increasing to mid-MIS 8, followed by low values at the end of MIS 8. Elevated EBFOI values typify MIS 7 with maxima at MIS 7e and 7a. In contrast, suboxic conditions prevailed during the MIS 7d stadial and MIS 6. MIS 5e is marked by relatively high EBFOI values, decreasing to MIS 5d. Following MIS 5, EBFOI values increased up to the Holocene, with maxima during MIS 3 and 1 and minima during MIS 4 and the LGM. Thus, EBFOI variability broadly follows glacial-interglacial cyclicity.

4.5. Benthic foraminiferal carbon isotope variability

In general, $\delta^{13}C$ values of the epifaunal group (*Cibicides* spp. and *Cibicidoides* spp.) are constantly heavier than infaunal taxa (*Cassidulina laevigata* and *Bulimina marginata*) (Fig. 6) (see Supplementary Material S2). This offset in carbon isotope values between epifaunal and infaunal has previously been demonstrated by Corliss (1985), Mojtahid et al. (2017), and Zahn et al. (1986). Lighter benthic infaunal $\delta^{13}C$ values correspond to intervals with high %NP (Fig. 5), especially near the end of glacial stages, such as at MIS 10, 8, 7d, 6 and 2 when the polar front was south of DSDP Site 548. In contrast, heavier $\delta^{13}C$ values occur during interglacial (MIS 11c, 9e, 7e, and 5e) and interstadial (MIS 5c, 5a, 3 and MIS 1) periods (Fig. 5).

5. Interpretation and discussion

5.1. DSDP Site 548 age model comparison

%NP data at DSDP Site 548 plotted using the new age model is comparable (Fig. 5) to other cores around the North Atlantic (Fig. 1). For example, climatic events such as MIS 7d are identified in DSDP 548 as a peak of %NP bounded by two %NP minima (MIS 7e and 7c) following the end of MIS 8 (Fig. 5), much like the observations from MD03–2692 (Bay of Biscay) (Mojtahid et al., 2005), ODP Site 983 (Barker et al., 2019), and Core M23414 (Rockall Plateau) (Kandiano, 2009) (Figs. 1, 7). Further, other significant climatic events, such as the warm MIS 9e interstadial and the southward polar front migration associated with the end of MIS 10 (Termination 4), are also observed in the %NP record of DSDP Site 548 (Fig. 7), suggesting that the new age model conforms to major climatic events around the area.

5.2. Benthic foraminiferal abundance and diversity

At DSDP Site 548, benthic foraminiferal abundance mirrors the phytodetritus sensitive group's abundance (Fig. 5), suggesting that increased organic matter fluxes to the seafloor contributed to the environment's ability to sustain larger populations. The relationship between benthic foraminiferal abundance and diversity to oxygen and nutrient availability is plotted using MINITAB statistical software to create contour maps, where the Y-axis indicates organic fluxes to the seafloor, the X-axis indicates dissolved oxygen concentration (Fig. 8),

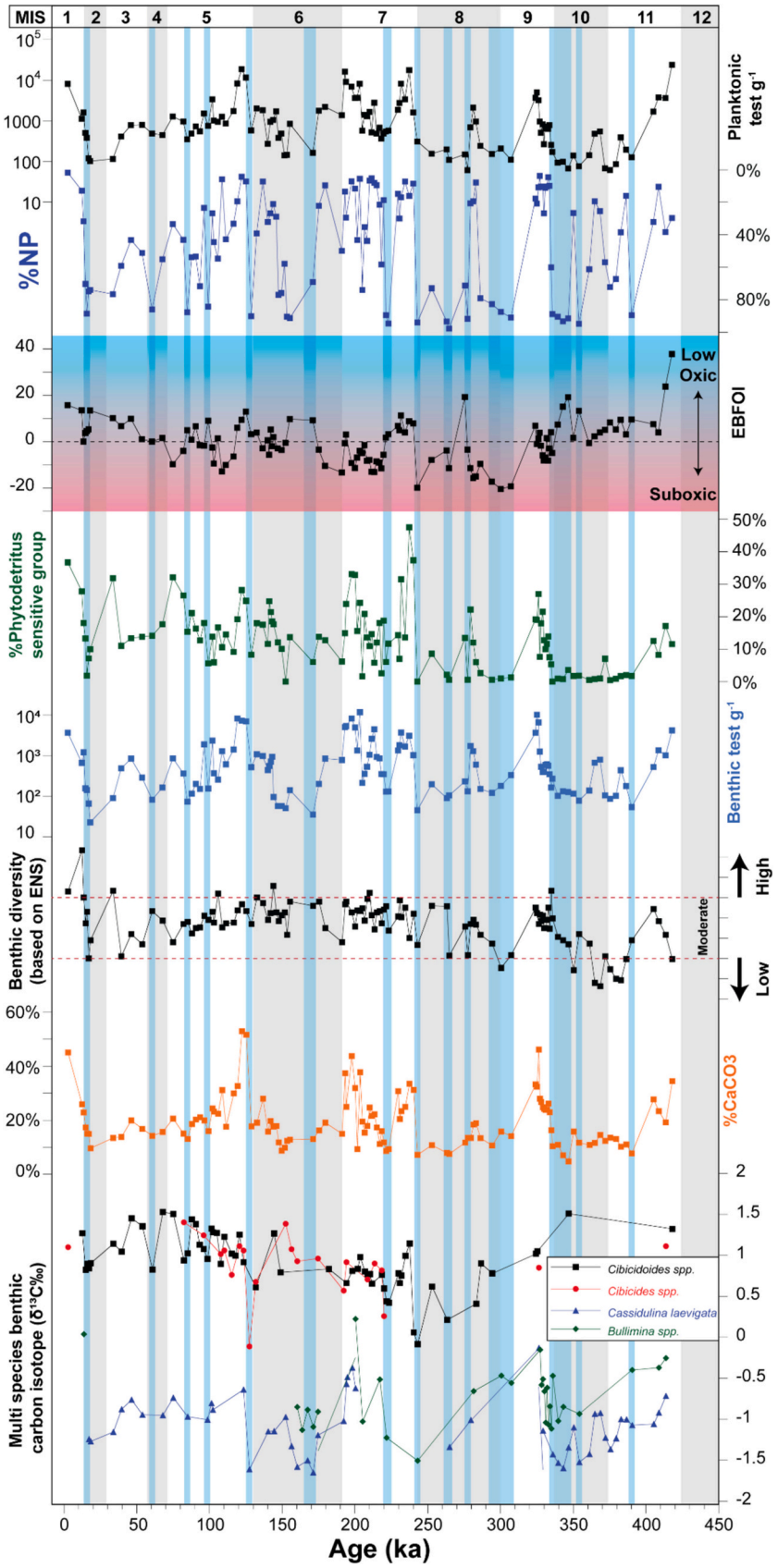

Fig. 5. Relationship between planktonic foraminifera abundance, %NP, EBFOI value, abundance of the phytodetritus group, %$CaCO_3$ benthic foraminiferal diversity, abundance, and $\delta^{13}C$ values at DSDP Site 548. Light blue vertical bars indicate periods when the polar front was south of DSDP 548, and light grey vertical bars indicate even-numbered MIS. (For interpretation of the references to colour in this figure legend, the reader is referred to the web version of this article.)

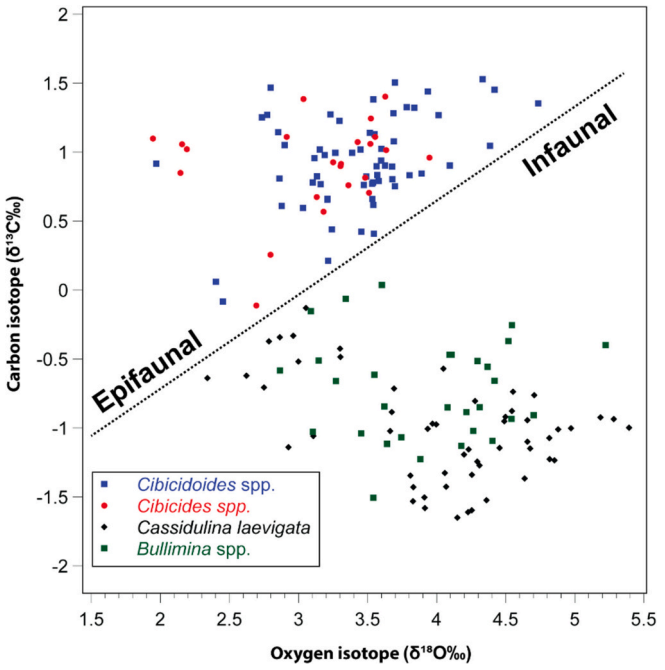

Fig. 6. The relationship between stable isotope composition of the benthic infaunal and epifaunal taxa at DSDP Site 548.

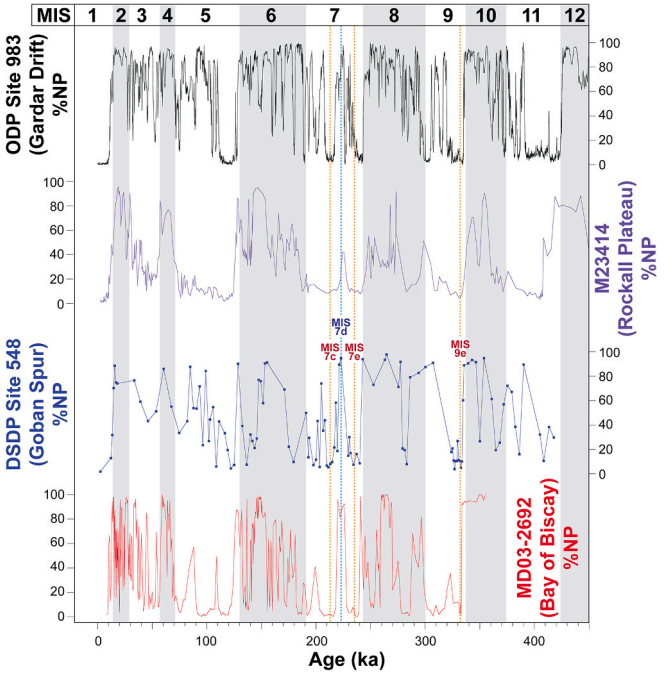

Fig. 7. %NP comparison between cores MD03–2692 (Mojtahid et al., 2005), M23414 (Kandiano, 2009), ODP Site 983 (Barker et al., 2019), and DSDP Site 548 (this work).

and the shaded areas indicate interpolated common z-axis values indicating benthic foraminiferal abundance (Fig. 8 A) or qualitative measures of benthic foraminiferal diversity (Fig. 8 B). In general, benthic foraminiferal diversity and abundance match dissolved oxygen concentration and organic matter fluxes. In contrast, minimal oxygen and nutrients result in low benthic foraminiferal abundance and diversity, with *C. laevigata* dominating the benthic assemblage when the dissolved oxygen reaches "low oxic" levels and common *Bolivina* spp. and *Bulimina marginata* if the dissolved oxygen level is within the "suboxic" level. High abundance- low diversity assemblages are dominated by *Globocassidulina subglobosa* and are associated with increased dissolved oxygen accompanied by low to moderate organic carbon flux. The low diversity of this assemblage may be explained by reduced oxygen and nutrient penetration to the sediment due to the high number of epifaunal *G. subglobosa* on the surface sediment, which consumes most of the available resources. This mechanism is one possible explanation for the relatively high variance between the abundance of *G. subglobosa* and other high dissolved oxygen indicator species (Fig. 4), particularly during strong interglacial conditions when environmental changes such as the invigoration of the Mediterranean Outflow Water (Kaboth et al., 2017) promote the dominance of *G. subglobosa* in the benthic foraminiferal assemblage. Lastly, high diversity assemblage is associated with moderately high levels of nutrients and oxygenation and is dominated by the phytodetritus group, suggesting an environment with a more diverse range of microhabitats for benthic foraminifers (Jorissen et al., 1995; Kranner et al., 2022).

There is a strong negative correlation (R^2 = 0.59) between the relative abundance of the polar planktonic species *Neogloboquadryina pachyderma* (%NP) and benthic foraminiferal abundance (Fig. 9), suggesting a relationship between sea surface temperature and export productivity. In general, benthic foraminiferal abundance was low during the colder periods when the polar front was south of DSDP Site 548 (Fig. 5), with benthic foraminifera concentrations varying from 100 to 1000 shells per gram. In contrast, during the warmer periods associated with low (<10 %) %NP, benthic abundance could reach a maximum of over 10,000 shells per gram. This pattern suggests that the dominance of the polar water during colder intervals limited surface water productivity (cf. van Kreveld 1996), reducing organic flux to the seafloor and limiting benthic foraminiferal abundance.

5.3. History of bottom water oxygenation and organic carbon flux variability at the Goban Spur over the last 400 ka

The relationship between planktonic foraminifera abundance, EBFOI value, the abundance of the phytodetritus group, benthic diversity (ENS), benthic foraminiferal abundance and %CaCO3 at DSDP Site 548 for the past 420,000 years are illustrated in (Fig. 5). EBFOI values and the abundance of the phytodetritus group reached a maximum during MIS 11, decreasing at the start of MIS 10. The oxic benthic taxon *G. subglobosa* dominates from ~417 to ~390 ka. Maximum benthic diversity was at ~405 ka, with high EBFOI values and the abundance of the phytodetritus group. At ~390 ka (MIS 11b), dysoxic taxa dominated when the polar front was south of DSDP Site 548 (Fig. 5). Minimal benthic and planktic foraminiferal abundance, lower diversity, rare phytodetritus taxa, and low $\%CaCO_3$ typified this cold interval. The cold period at ~390 ka corresponds to a %NP maximum at ODP Site 983 (Barker et al., 2019) and ODP Site 980 (Oppo et al., 1998), suggesting a cold event across the North Atlantic.

Benthic foraminiferal assemblages at DSDP Site 548 suggest reduced bottom water ventilation and organic matter flux to the seafloor from the peak MIS 11 interglacial conditions to the colder MIS 10. In addition, a lower $\%CaCO_3$ concentration during this time likely indicates reduced MOW intensity, causing the facies to transition from calcareous silt to mud. Kaboth et al. (2017) interpreted a similar facies transition at IODP Site U1386 in the Gulf of Cadiz (Fig. 1) from MIS 11 to MIS 10 and suggested this was related to the progressive weakening of bottom currents related to a less active Mediterranean Outflow Water. The taxon *C. laevigata* dominates throughout MIS 10 when the abundance of the phytodetritus group is low, and EBFOI values suggest "low oxic" levels until the end of the stage.

Suboxic conditions prevailed from ~332 to ~330 ka and at ~324 ka when foraminiferal abundance, diversity, the abundance of the phytodetritus group, and $\%CaCO_3$ were elevated in the calcareous silty-sand facies at DSDP Site 548. This suggests relatively well-ventilated bottom water with higher organic flux, likely related to a more vigorous

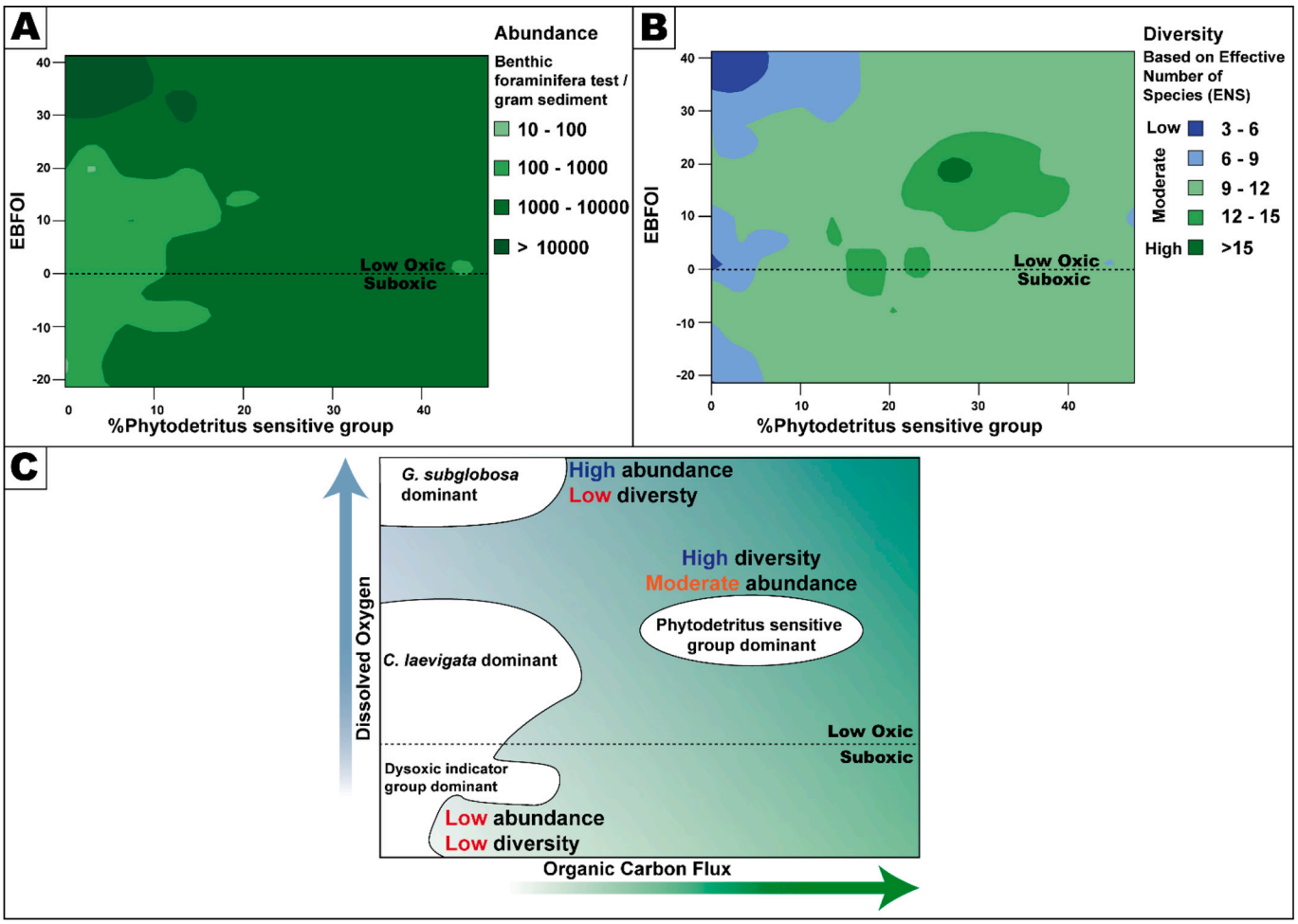

Fig. 8. A. Contour plots showing the relationship between EBFOI, phytodetritus taxa and benthic abundance. B: Contour plot indicating the relationship between EBFOI, the abundance of phytodetritus taxa and benthic diversity. C: Interpreted benthic assemblage classification and its relationship to nutrient, oxygen levels and benthic foraminiferal abundance and diversity.

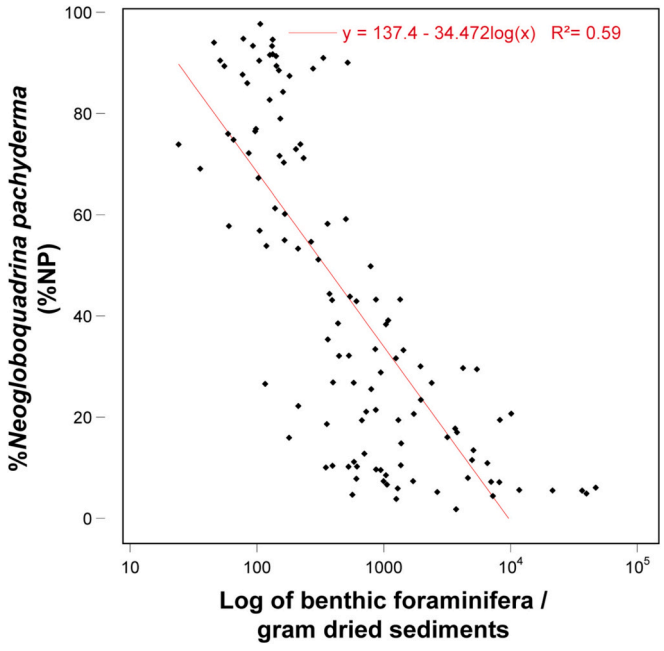

Fig. 9. Relationship between %NP and benthic foraminiferal abundance.

MOW during the warmer Purfleet (MIS 9) interglacial (Helmke and Bauch, 2003; Voelker et al., 2010). An equivalent, MOW-associated MIS 9 contourite deposit is also found in the Gulf Cadiz (Kaboth et al., 2017), suggesting that this MOW invigoration happened through most of its flow path along the Western European continental margin.

The climate shifted to a glacial mode during MIS 8 when the polar front migrated south of DSDP Site 548 by ~307 ka, associated with dysoxic bottom water conditions. This polar front migration event, however, did not reach MD03–2692 at the Bay of Biscay (Fig. 1) (Mojtahid et al., 2005), suggesting that the polar front was situated in between the two sites at ~307 ka. Subsequently, suboxic conditions prevailed during the rest of MIS 8. The abundance of the phytodetritus group is low except for a peak at ~279 ka, marked with increased benthic foraminifera abundance (Fig. 4). During Termination 3 at ~243 ka, EBFOI values, the abundance of the phytodetritus group, and benthic foraminiferal abundance were low. This suggests low dissolved oxygen and nutrients, possibly related to increased meltwater input associated with the collapse of the MIS 8 BIIS, as suggested by the high %NP and IRD concentration at DSDP Site 548 (Fabian et al., 2023) and the Celtic Margin (Mojtahid et al., 2005).

Organic flux varied markedly throughout MIS 7, with peaks of benthic foraminifera yield during MIS 7e, c, and a interstadial condition (Fig. 5). A similar benthic foraminiferal abundance pattern is also observed in Core MD03–2692 at the Bay of Biscay (Mojtahid et al., 2005), suggesting a regional increase in primary productivity. In contrast, low abundance of the phytodetritus group was associated with

the stadial conditions during MIS 7d and, to a lesser extent, MIS 7b. From MIS 7e to MIS 7d, bottom water dissolved oxygen levels increased, followed by a return to suboxic levels near the end of MIS 7d or during Termination 3a, persisting until early MIS 6. By ~182 ka, the oxygenation level increased to low oxic levels.

"Low oxic" conditions prevailed until MIS 5e, rapidly decreasing to suboxic levels by MIS 5d. Subsequently, "low oxic" conditions continued until the Holocene. Organic flux reached a maximum during MIS 5e and MIS 5a associated with maxima in benthic and planktonic foraminiferal abundance, matching those observed at Core MD03–2692 (Mojtahid et al., 2005) and associated with the calcareous sandy-silt facies at DSDP Site 548 (Fig. 3), which matched the contourite sequences at IODP Site U1386 (Fig. 1) (Kaboth et al., 2017). The lowest phytodetritus abundance during MIS 5 is likely associated with a minor polar front excursion to the south of DSDP Site 548 at ~98 ka (Fig. 5).

Subsequently, the abundance of the phytodetritus group gradually decreased, reaching a minimum by 16.5 ka during the LGM (Last Glacial Maximum). The abundance of the phytodetritus group maximum at 33 ka was likely coeval to Heinrich Event 3 (HE 3). Previously, a benthic diversity minimum during the LGM was also described from MD03–2692 in the Bay of Biscay (Mojtahid et al., 2017), possibly suggesting a benthic diversity minimum event along the Celtic Margin. After the LGM minima, oxygenation levels and benthic foraminiferal abundance increased from early MIS 1 to the present.

A model of the oceanographic conditions at the Goban Spur based on this study highlights the differences between warmer and colder climates over the last 420,000 years (Fig. 10). During warmer periods, such as the peaks of MIS 11 and 5e interglacial, high planktonic foraminiferal abundance suggest increased surface water primary productivity (Fig. 10). Further, these periods are also marked with increased organic material fluxes to the seafloor matched with increased benthic foraminiferal abundance (Fig. 5). Benthic foraminiferal diversity, however, is also influenced by the amount of dissolved oxygen, as evident from the lower diversity horizons dominated by *Globocassidulina subglobosa* (Figs. 5, 8 C) during MIS 11. Further, lighter benthic $\delta^{13}C$ and increased $\%CaCO_3$ (Fig. 5), possibly associated with increased biogenic calcareous material deposition and fine particle winnowing by a more vigorous MOW regime subsequently forming sandy contourite sequences (Kaboth et al., 2017; Fabian et al., 2023), also characterises the warmer periods at DSDP Site 548. Conversely, during the colder climate of glacial periods, low-productivity and cold polar water, marked by *N. pachyderma* dominant planktonic foraminifera assemblage, dominates the surface water mass of the Goban Spur (Fabian et al., 2023), which resulted in less organic fluxes to the seafloor (Fig. 10), possibly contributing to lower benthic foraminiferal abundance. Heavier benthic $\delta^{13}C$ (Fig. 5) also characterises the colder period at the Goban Spur. The dominant benthic foraminifera taxa are dependent on the amount of dissolved oxygen on the seafloor. When the dissolved oxygen is below 0.3 mL/L, the benthic assemblage is dominated by the dysoxic group, and the oligotrophic tolerant *Cassidulina laevigata* becomes more common as the concentration of dissolved oxygen increases (Fig. 8 C).

6. Conclusion

Benthic foraminiferal assemblage, stable isotope data and facies of DSDP Site 548 are used to interpret the Quaternary bottom water ventilation, organic flux, and bottom current variability at the Goban Spur. The correlation between benthic $\delta^{18}O$ to the LR04 curve (Lisiecki and Raymo, 2005) combined with %NP data and IRD concentration comparison to other North Atlantic cores extends the DSDP Site 548 age model of Fabian et al. (2023) to span the past 420,000 years. Benthic foraminiferal assemblages at DSDP Site 548 differ significantly between the glacial and interglacial intervals. Glacial intervals are marked with lower benthic foraminiferal abundance and diversity, lighter $\delta^{13}C$ and low $\%CaCO_3$ values. These periods are dominated by either *Cassidulina laevigata* or low dissolved oxygen indicator taxa such as *Bolivina* spp. and *Globobulimina* spp., particularly when the polar front was south of DSDP Site 548 (>80 %NP). Further, low planktonic foraminiferal abundance and the dominance of *Neogloboquadrina pachyderma* suggest the prevalence of lower primary productivity in polar water at the surface, alluding to more limited organic fluxes to the seafloor. In addition, the lower dissolved oxygen concentration likely limits the range of viable benthic microhabitats, consequently lowering benthic foraminiferal abundance and diversity. In contrast, interglacial intervals, especially during MIS 11, are marked by the dominance of the high dissolved oxygen indicator species, such as *Globocassidulina subglobosa,* while phytodetritus sensitive taxa, such as *Epistominella exigua* and *Alabaminella weddellensis*, dominate younger interglacial and interstadial intervals, such as during MIS 7e, 5a, and 3, suggesting a better ventilated bottom water. Higher planktonic foraminiferal abundance suggests the presence of higher productivity surface water, contributing to higher levels of organic fluxes and, consequently, higher benthic foraminiferal

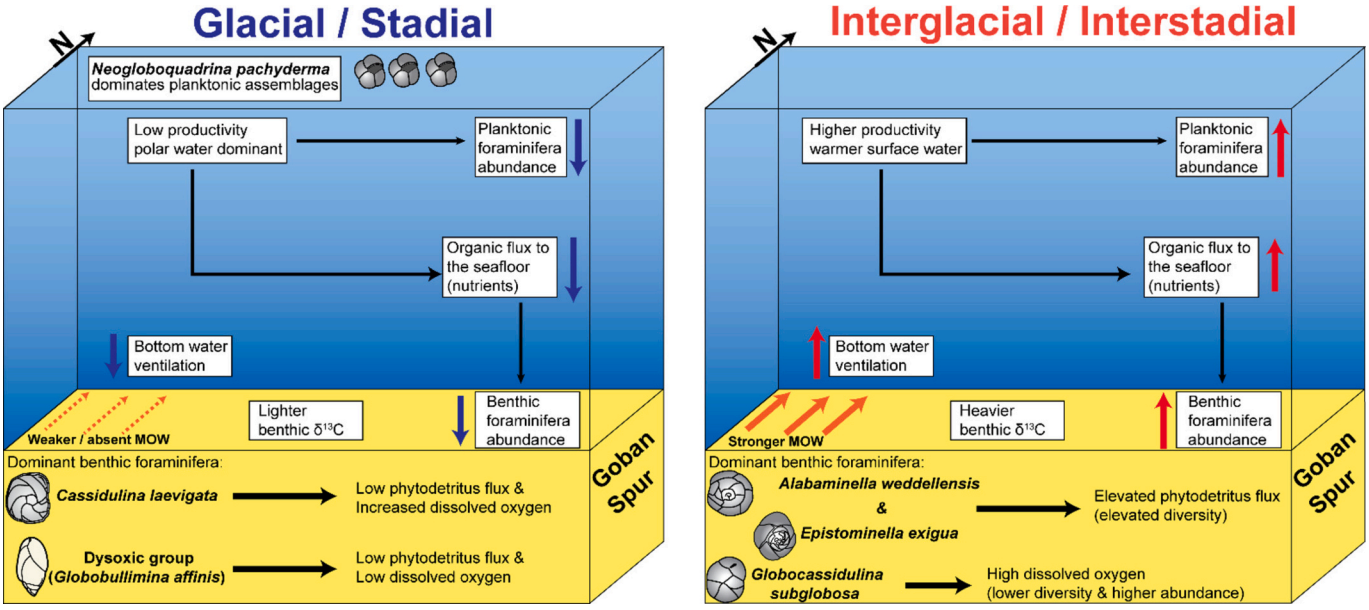

Fig. 10. A model contrasting the glacial and interglacial oceanographic conditions at the Goban Spur.

abundance. Further, the warmer periods at DSDP Site 548 for the past 420,000 years are also marked with high %$CaCO_3$ and lighter $\delta^{13}C$, possibly associated with the invigoration of the MOW.

Author contribution

SJG and SGF conceived the study. SGF led the sample collection, preparation, and analyses, along with data acquisition, synthesis and manuscript writing, with guidance from SJG and DDV. DDV wrote the 'Benthic foraminifera stable isotope analysis' in section 3.3 and provided stable isotope measurements from samples prepared by SGF. SGF revised the final manuscript by incorporating inputs from SJG and DDV.

Author statement

All authors have approved the manuscript and agree with its submission to *Marine Micropaleontology*.

This manuscript has not been published, nor is it under consideration by any other journal.

CRediT authorship contribution statement

Stanislaus Glenndy Fabian: Writing – review & editing, Writing – original draft, Visualization, Methodology, Investigation, Formal analysis, Data curation, Conceptualization. **Stephen J. Gallagher:** Writing – review & editing, Supervision, Conceptualization. **David De Vleeschouwer:** Methodology, Data curation.

Declaration of competing interest

The authors declare that they have no known competing financial interests or personal relationships that could have appeared to influence the work reported in this paper.

Acknowledgements

An Australian Government Research Training Program Scholarship supports Stanislaus G. Fabian. Funding was provided to SJG by the Australian IODP office. The authors thank the IODP Bremen Core Repository for granting access to inspect and sample DSDP Core 548. Thanks are due to Artur Fugmann for laboratory assistance and support on the mass spectrometers at the University of Münster.

Appendix A. Supplementary data

Supplementary data to this article can be found online at https://doi.org/10.1016/j.marmicro.2024.102432.

Data availability

Data will be made available on request.

References

Barker, S., Knorr, G., Conn, S., Lordsmith, S., Newman, D., Thornalley, D.J.R., 2019. Foraminifer and IRD counts from ODP Site 162-983, Barker, S et al. (2019): early Interglacial Legacy of Deglacial climate Instability. Paleoceanogr. Paleoclimatol. 34 (8), 1455–1475. PANGAEA. https://doi.org/10.1594/PANGAEA.904398.

Bashirova, L.D., Kandiano, E.S., Sivkov, V.V., Bauch, H.A., 2014. Migrations of the North Atlantic Polar front during the last 300 ka: evidence from planktic foraminiferal data. Oceanology 54, 798–807. https://doi.org/10.1134/s0001437014060010.

Brückner, S., 2007. Climatic and Hydrographic Variability in the Late Holocene Skagerrak as Deduced from Benthic Foraminiferal Proxies, Fachbereich 05: Geowissenschaften (FB 05).. Universität Bremen, Bremerhaven, Germany www.nbn-resolving.de/urn:nbn:de:gbv:46-diss000109893.

Clemens, S.C., Prell, W.L., Howard, W.R., 1987. Retrospective dry bulk density estimates from Southeast Indian Ocean sediments—comparison of water loss and chloride-ion methods. Mar. Geol. 76, 57–69. https://doi.org/10.1016/0025-3227(87)90017-x.

Corliss, B.H., 1985. Microhabitats of benthic foraminifera within deep-sea sediments. Nature 314 (6010), 435–438. https://doi.org/10.1038/314435a0.

De Graciansky, P.C., Poag, C., Cunningham, R., Loubere, P., Masson, D., Mazzullo, J., Montadert, L., Müller, C., Otsuka, K., Reynolds, L., 1985a. Site 548. Initial Rep. Deep Sea Drill. Proj. 80, 33–122. https://doi.org/10.2973/dsdp.proc.80.103.1985.

De Graciansky, P.C., Poag, C.W., Foss, G., 1985b. Drilling on the Goban Spur-objectives, regional geological setting, and operational summary. Initial Rep. Deep Sea Drill. Proj. 80, 5–13. https://doi.org/10.2973/dsdp.proc.80.101.1985.

Delivet, S., Van Eetvelt, B., Monteys, X., Ribó, M., Van Rooij, D., 2016. Seismic geomorphological reconstructions of Plio-Pleistocene bottom current variability at Goban Spur. Mar. Geol. 378, 261–275. https://doi.org/10.1016/j.margeo.2016.01.001.

Depuydt, P., Mojtahid, M., Barras, C., Bouhdayad, F.Z., Toucanne, S., 2022. Intermediate Ocean circulation and cryosphere dynamics in the Northeast Atlantic during Heinrich Stadials: benthic foraminiferal assemblage response. J. Quat. Sci. 37, 1207–1221. https://doi.org/10.1002/jqs.3444.

Depuydt, P., Barras, C., Toucanne, S., Fossile, E., Mojtahid, M., 2023. Implication of size fraction on benthic foraminiferal-based paleo-reconstructions: a case study from the Bay of Biscay (NE Atlantic). Mar. Micropaleontol. 181. https://doi.org/10.1016/j.marmicro.2023.102242.

Diz, P., Hall, I.R., Zahn, R., Molyneux, E.G., 2007. Paleoceanography of the southern Agulhas Plateau during the last 150 ka: Inferences from benthic foraminiferal assemblages and multispecies epifaunal carbon isotopes. Paleoceanography 22. https://doi.org/10.1029/2007pa001511.

Eynaud, F., de Abreu, L., Voelker, A., Schönfeld, J., Salgueiro, E., Turon, J.-L., Penaud, A., Toucanne, S., Naughton, F., Sánchez Goñi, M.F., Malaizé, B., Cacho, I., 2009. Position of the Polar Front along the western Iberian margin during key cold episodes of the last 45 ka. Geochem. Geophys. Geosyst. 10. https://doi.org/10.1029/2009gc002398.

Fabian, S.G., Gallagher, S.J., De Vleeschouwer, D., 2023. British–Irish Ice Sheet and polar front history of the Goban Spur, offshore southwest Ireland over the last 250 000 years. Boreas 52, 476–497. https://doi.org/10.1111/bor.12631.

Fontanier, C., 2006. Seasonal Variability of Benthic Foraminiferal Faunas at 1000 M Depth in the Bay of Biscay. J. Foraminiferal Res. 36, 61–76. https://doi.org/10.2113/36.1.61.

Gonthier, E.G., Faugères, J.C., Stow, D.A.V., 1984. Contourite facies of the Faro Drift, Gulf of Cadiz. Geol. Soc. Lond. Spec. Publ. 15, 275–292. https://doi.org/10.1144/GSL.SP.1984.015.01.18.

Gooday, A.J., 1993. Deep-sea benthic foraminiferal species which exploit phytodetritus: characteristic features and controls on distribution. Mar. Micropaleontol. 22, 187–205. https://doi.org/10.1016/0377-8398(93)90043-w.

Helmke, J.P., Bauch, H.A., 2003. Comparison of glacial and interglacial conditions between the polar and subpolar North Atlantic region over the last five climatic cycles. Paleoceanography 18. https://doi.org/10.1029/2002pa000794.

Hulsemann, J., 1966. On the routine analysis of carbonates in unconsolidated sediments. J. Sediment. Res. 36 www.pubs.geoscienceworld.org/sepm/jsedres/article/36/2/622/95929/on-the-routine-analysis-of-carbonates-in.

Jorissen, F.J., de Stigter, H.C., Widmark, J.G., 1995. A conceptual model explaining benthic foraminiferal microhabitats. Mar. Micropaleontol. 26, 3–15. https://doi.org/10.1016/0377-8398(95)00047-x.

Jost, L., 2006. Entropy and diversity. Oikos 113, 363–375. https://doi.org/10.1111/j.2006.0030-1299.14714.x.

Kaboth, S., de Boer, B., Bahr, A., Zeeden, C., Lourens, L.J., 2017. Mediterranean Outflow Water dynamics during the past~ 570 kyr: Regional and global implications. Paleoceanography 32, 634–647. https://doi.org/10.1002/2016pa003063.

Kaboth-Bahr, S., Bahr, A., Zeeden, C., Toucanne, S., Eynaud, F., Jiménez-Espejo, F., Röhl, U., Friedrich, O., Pross, J., Löwemark, L., 2018. Monsoonal forcing of European ice-sheet dynamics during the late Quaternary. Geophys. Res. Lett. 45, 7066–7074. https://doi.org/10.1029/2018gl078751.

Kaiho, K., 1994. Benthic foraminiferal dissolved-oxygen index and dissolved-oxygen levels in the modern ocean. Geology 22, 719–722. https://doi.org/10.1130/0091-7613(1994)022<0719:bfdoia>2.3.co;2.

Kandiano, E.S., 2009. (Table a.01) Planktic foraminiferal census data of sediment core GIK23414-9, Kandiano.

Kranner, M., Harzhauser, M., Beer, C., Auer, G., Piller, W.E., 2022. Calculating dissolved marine oxygen values based on an enhanced Benthic Foraminifera Oxygen Index. Sci. Rep. 12, 1–13. https://doi.org/10.1038/s41598-022-05295-8.

Kucera, M., 2007. Chapter six Planktonic Foraminifera as Tracers of Past Oceanic Environments. In: Hillaire-Marcel, C., De Vernal, A. (Eds.), Proxies in late Cenozoic Paleoceanography, pp. 213–262. https://doi.org/10.1016/s1572-5480(07)01011-1.

Lear, C.H., Coxall, H.K., Foster, G.L., Lunt, D.J., Mawbey, E.M., Rosenthal, Y., Sosdian, S. M., Thomas, E., Wilson, P.A., 2015. Neogene ice volume and ocean temperatures: Insights from infaunal foraminiferal Mg/ca paleothermometry. Paleoceanography 30, 1437–1454. https://doi.org/10.1002/2015pa002833.

Lisiecki, L.E., Raymo, M.E., 2005. A Pliocene-Pleistocene stack of 57 globally distributed benthic δ18O records. Paleoceanography 20. https://doi.org/10.1029/2004pa001071.

Mojtahid, M., Eynaud, F., Zaragosi, S., Scourse, J., Bourillet, J.F., Garlan, T., 2005. Palaeoclimatology and palaeohydrography of the glacial stages on Celtic and Armorican margins over the last 360000 yrs. Mar. Geol. 224, 57–82. https://doi.org/10.1016/j.margeo.2005.07.007.

Mojtahid, M., Toucanne, S., Fentimen, R., Barras, C., Le Houedec, S., Soulet, G., Bourillet, J.-F., Michel, E., 2017. Changes in Northeast Atlantic hydrology during termination 1: Insights from Celtic margin's benthic foraminifera. Quat. Sci. Rev. 175, 45–59. https://doi.org/10.1016/j.quascirev.2017.09.003.

Murray, J.W., 2006. Ecology and Applications of Benthic Foraminifera. Cambridge University Press, Cambridge. https://doi.org/10.1017/CBO9780511535529.
Oppo, D.W., McManus, J.F., Cullen, J.L., 1998. Abrupt climate events 500,000 to 340,000 years ago: evidence from subpolar North Atlantic sediments. Science 279, 1335–1338. https://doi.org/10.1126/science.279.5355.1335.
O'Reilly, L., Fentimen, R., Butschek, F., Titschack, J., Lim, A., Moore, N., O'Connor, O.J., Appah, J., Harris, K., Vennemann, T., Wheeler, A.J., 2022. Environmental forcing by submarine canyons: evidence between two closely situated cold-water coral mounds (Porcupine Bank Canyon and Western Porcupine Bank, NE Atlantic). Mar. Geol. 454, 106930. https://doi.org/10.1016/j.margeo.2022.106930.
Railsback, L.B., Gibbard, P.L., Head, M.J., Voarintsoa, N.R.G., Toucanne, S., 2015. An optimized scheme of lettered marine isotope substages for the last 1.0 million years, and the climatostratigraphic nature of isotope stages and substages. Quaternary Science Reviews 111, 94–106. https://doi.org/10.1016/j.quascirev.2015.01.012.
Rice, A., Thurston, M., Bett, B., 1994. The IOSDL DEEPSEAS programme: introduction and photographic evidence for the presence and absence of a seasonal input of phytodetritus at contrasting abyssal sites in the northeastern Atlantic. Deep-Sea Res. I Oceanogr. Res. Pap. 41, 1305–1320. https://doi.org/10.1016/0967-0637(94)90099-x.
Rüggeberg, A., Dullo, C., Dorschel, B., Hebbeln, D., 2007. Environmental changes and growth history of a cold-water carbonate mound (Propeller Mound, Porcupine Seabight). Int. J. Earth Sci. 96, 57–72. https://doi.org/10.1007/s00531-005-0504-1.
Saraswat, R., Deopujari, A., Nigam, R., Heniriques, P.J., 2011. Relationship between abundance and morphology of benthic foraminifera Epistominella exigua: Paleoclimatic implications. J. Geol. Soc. India 77, 190–196. https://doi.org/10.1007/s12594-011-0014-7.
Schlitzer, R., 2023. Ocean Data View. www.odv.awi.de.
Schnitker, D., 1980. Quaternary deep-sea benthic foraminifers and bottom water masses. Annu. Rev. Earth Planet. Sci. 8, 343–370. https://doi.org/10.1146/annurev.ea.08.050180.002015.
Schönfeld, J., 1997. The impact of the Mediterranean Outflow Water (MOW) on benthic foraminiferal assemblages and surface sediments at the southern Portuguese continental margin. Mar. Micropaleontol. 29, 211–236. https://doi.org/10.1016/s0377-8398(96)00050-3.
Schönfeld, J., 2002. A new benthic foraminiferal proxy for near-bottom current velocities in the Gulf of Cadiz, northeastern Atlantic Ocean. Deep-Sea Res. I Oceanogr. Res. Pap. 49, 1853–1875. https://doi.org/10.1016/s0967-0637(02)00088-2.
Schönfeld, J., Zahn, R., 2000. Late Glacial to Holocene history of the Mediterranean Outflow. Evidence from benthic foraminiferal assemblages and stable isotopes at the Portuguese margin. Palaeogeogr. Palaeoclimatol. Palaeoecol. 159, 85–111. https://doi.org/10.1016/s0031-0182(00)00035-3.
Schönfeld, J., Dullo, W.-C., Pfannkuche, O., Freiwald, A., Rüggeberg, A., Schmidt, S., Weston, J., 2010. Recent benthic foraminiferal assemblages from cold-water coral mounds in the Porcupine Seabight. Facies 57, 187–213. https://doi.org/10.1007/s10347-010-0234-0.
Sun, X., Corliss, B.H., Brown, C.W., Showers, W.J., 2006. The effect of primary productivity and seasonality on the distribution of deep-sea benthic foraminifera in the North Atlantic. Deep-Sea Res. I Oceanogr. Res. Pap. 53, 28–47. https://doi.org/10.1016/j.dsr.2005.07.003.
Thomas, E., Gooday, A.J., 1996. Cenozoic deep-sea benthic foraminifers: tracers for changes in oceanic productivity? Geology 24, 355–358. https://doi.org/10.1130/0091-7613(1996)024<0355:cdsbft>2.3.co;2.
Thomas, E., Booth, L., Maslin, M., Shackleton, N.J., 1995. Northeastern Atlantic benthic foraminifera during the last 45,000 years: changes in productivity seen from the bottom up. Paleoceanography 10, 545–562. https://doi.org/10.1029/94pa03056.
Turner, J.T., 2015. Zooplankton fecal pellets, marine snow, phytodetritus and the ocean's biological pump. Prog. Oceanogr. 130, 205–248. https://doi.org/10.1016/j.pocean.2014.08.005.
van Kreveld, S.A., 1996. Northeast Atlantic late Quaternary planktic foraminifera as primary productivity and water mass indicators. Scr. Geol. 113, 23–91. www.repository.naturalis.nl/pub/317525/SG1996113002.pdf.
Vázquez Riveiros, N., Govin, A., Waelbroeck, C., Mackensen, A., Michel, E., Moreira, S., Bouinot, T., Caillon, N., Orgun, A., Brandon, M., 2016. Mg/ca thermometry in planktic foraminifera: improving paleotemperature estimations for G. Bulloides and N. Pachyderma left. Geochem. Geophys. Geosyst. 17, 1249–1264. https://doi.org/10.1002/2015gc006234.
Voelker, A.H.L., Rodrigues, T., Billups, K., Oppo, D., McManus, J., Stein, R., Hefter, J., Grimalt, J.O., 2010. Variations in mid-latitude North Atlantic surface water properties during the mid-Brunhes (MIS 9–14) and their implications for the thermohaline circulation. Clim. Past 6, 531–552. https://doi.org/10.5194/cp-6-531-2010.
Wallace, M.W., Holdgate, G.R., Daniels, J., Gallagher, S.J., Smith, A., 2002. Sonic velocity, submarine canyons, and burial diagenesis in oligocene-holocene cool-water carbonates, gippsland basin, Southeast Australia. AAPG Bull. 86, 1593–1607. https://doi.org/10.1306/61eedd14-173e-11d7-8645000102c1865d.
Zahn, R., Winn, K., Sarnthein, M., 1986. Benthic foraminiferal δ13C and accumulation rates of organic carbon: Uvigerina peregrina group and Cibicidoides wuellerstorfi. Paleoceanography 1, 27–42. https://doi.org/10.1029/pa001i001p00027.